

# Ice cover, winter circulation, and exchange in Saginaw Bay and Lake Huron

Tuan D. Nguyen,<sup>1\*</sup> Nathan Hawley,<sup>2</sup> Mantha S. Phanikumar<sup>1</sup>

<sup>1</sup>Department of Civil and Environmental Engineering, Michigan State University, East Lansing, Michigan

<sup>2</sup>NOAA Great Lakes Environmental Research Laboratory, Ann Arbor, Michigan

## Abstract

Winter circulation exerts a strong control on the release and timing of nutrients and contaminants from bays into the adjoining lakes. To estimate winter residence times of solutes in the presence of ice cover, we used an ice model coupled to hydrodynamic, thermal and solute transport models of Saginaw Bay and Lake Huron for two low (2010 and 2013) and two high (2009 and 2014) ice years. The models were tested using temperature data from thermistor chains and current data from ADCP moorings deployed during the winter-time. Simulated water temperatures compared favorably to lake-wide average surface temperatures derived from NOAA's AVHRR satellite imagery. Simulated results of ice cover are in agreement with observed data from the Great Lakes Ice Atlas. Our results indicate that ice cover significantly dampens water movement producing almost stagnant conditions around February. Estimates of residence times for Saginaw Bay (defined as the e-folding flushing time based on vertically integrated dye concentrations) show that the mean residence times in a low ice year (2013) are 2.2 months for the inner bay, and 3.5 months for the entire bay. The corresponding numbers for a high ice year (2014) are 4.9 and 5.3 months, respectively. Considering the entire bay, solutes stored in the bay can be expected to be released into the lake between March (low ice year) and April (high ice year). These results are expected to aid in understanding the behavior of contaminants in the Great Lakes during the winter months and in early spring.

Ice processes, winter circulation and thermal structure in lakes and oceans have attracted significant attention in recent years (Wang et al. 2010; Gao et al. 2011; Fujisaki et al. 2012, 2013; Oveisy et al. 2012; Rizk et al. 2014; Titze and Austin 2014; Urrego-Blanco and Sheng 2014; Van Cleave et al. 2014; Wang et al. 2014). The presence of ice in bays and over lakes can significantly modify circulation, thermal structure, and the residence times of contaminants, and wind-driven ice floes are known to be a hazard to beach front homes (Gilchrist and LaLonde 2009).

The limited literature on the winter circulation of Lake Huron includes information on the extent of ice cover since the annual cycles of ice formation and loss affect the physical and ecosystem processes within the lake (Assel 2005). Because of isothermal conditions in the water column, winter currents are barotropic (Beletsky et al. 1999). However, accurate simulation of currents under winter conditions continues to be a challenge for a number of reasons. The

difficulties come from not only a lack of high-quality observations during the wintertime but are also due to the coupled nature of the complex processes involved. Ice cover, for example, is a primary factor that inhibits the downward propagation of the surface wind stress into the water column (Wang et al. 2010) thus influencing lake circulation, which in turn, affects the growth and movement of ice. One of the first attempts to describe winter circulation in Lake Huron was carried out by Saylor and Miller (1979), who deployed 21 current moorings in Lake Huron for approximately 6 months during the winter of 1974–1975. They concluded that there is a strong cyclonic flow throughout the winter with current speeds that ranged from 1 to 7 cm/s with a mean of 3 cm/s. Fujisaki et al. (2012) used the Princeton Ocean Model (POM) with ice processes to investigate the seasonal variation of ice cover on Lake Erie. The study showed that the packed ice cover slowed down surface water velocities. To simulate ice processes and circulation in Lake Erie, Wang et al. (2010) developed the Great Lakes ice-circulation model (GLIM) based on a combination of the Coupled Ice Ocean Model (CIOM) and the Great Lakes version of the Princeton Ocean Model (POM). Bai et al. (2013) conducted the first simulation of Great Lakes circulation without ice

\*Correspondence: nguy236@egr.msu.edu

Additional Supporting Information may be found in the online version of this article.

using FVCOM. Their results for circulation show the existence of a large cyclonic cell in Lake Huron.

The mechanisms that drive hydrodynamic exchange between Saginaw Bay and Lake Huron have not been fully understood. For example, Nguyen et al. (2014) pointed out the important role played by cyclonic gyres in Saginaw Bay and their role in influencing the residence times of solutes within the bay. Quantifying winter residence times is challenging due to the presence of ice and complex spatiotemporal variations of wind stress over the lake. The Laurentian Great Lakes are ice-covered to some extent each winter so these changes occur on an annual basis. These lakes have considerable influence on the regional climate (Bates et al. 1993; Scott and Huff 1996), which in turn influences circulation and thermal structure. Regime shifts in the Great Lakes water balance following the warm El Niño winter of 1997–1998 were noted recently (Gronewold and Stow 2014; Van Cleave et al. 2014) and the lowest ever recorded water levels in the Lake Michigan–Lake Huron system occurred in January 2013 (Gronewold and Stow 2014). Recent water level declines and water quality issues in the Great Lakes have made it necessary to estimate storage changes on land (Niu et al. 2014) and within the lakes (Nguyen et al. 2014; Nguyen 2014), so knowledge of water movement and temperature distribution during winter months are of critical importance to a number of questions related to the Great Lakes in general, and to Lake Huron and Saginaw Bay in particular.

The hydrology of the Great Lakes can also affect local meteorological conditions in the long term. Scott and Huff (1996) estimated that lake-effect precipitation increased 90% downwind of Lake Huron in the wintertime; therefore, understanding the major effects of colder weather on the lake is crucial to predicting water movement patterns and water temperature structure. Ice cover is also an important indicator of regional climate change (Robertson et al. 1992). In a study related to the trends of ice cover in the Great Lakes, Assel et al. (2003) pointed out that the distributions of ice cover among the five Laurentian Great Lakes were influenced by the spatial pattern of water depth in each lake and by regional differences in air temperature.

Recent research links algal blooms in mid-winter and early spring to conditions such as residence time during winter. Twiss et al. (2014) found that the growth and loss rates of phytoplankton during mid-winter (with full ice cover) in Lake Erie are as high as the values observed in summer with no net growth occurring. Zero net growth implies that the plankton are stored in a state of static biomass during winter and that these remnants from previous blooms could contribute to large portions of accumulated phytoplankton observed in February. This suggests that winter residence times of solutes in bays connected to the Great Lakes may be a factor in explaining the timing of algal blooms in the lakes during winter and early spring; however, there are gaps in

our understanding of winter limnology and estimates of residence times during the winter are not available. There are a few studies on water exchange between Saginaw Bay and Lake Huron and residence times in Saginaw Bay (Dolan 1975; Nguyen et al. 2014) but the estimates were made for the summer time.

The primary objective of the present paper is to describe winter circulation, ice cover and thermal structure of Lake Huron in response to recent wintertime meteorological conditions. A second major objective is to obtain estimates of the residence time and flushing time for Saginaw Bay in the presence of ice cover and to understand the variability in winter residence times between low and high ice cover years. This variability is key to explaining the timing of when dissolved and suspended material stored in the bay over the winter are expected to be released into the lake. In this study, the simulated currents, temperatures, and ice covers are compared to available observational data, and spatial maps of the surface temperature, ice concentration, and ice thickness are presented for four winters (2008–2009, 2009–2010, 2012–2013, and 2013–2014). The flushing times and residence times for Saginaw Bay are estimated and compared to the corresponding values in summer seasons calculated by Nguyen et al. (2014). The annual maximum ice coverage over the Great Lakes was about 72% (2009), 26.4% (2010), 38.4% (2013), and 92.5% (2014), so these winters are considered low ice cover (2010 and 2013) and high ice cover (2009 and 2014) respectively when compared to available data for the 41-yr period 1974–2015, which has a long-term average of 53.2%.

## Material and methods

### Study site

Lake Huron (Fig. 1) is the third largest of the Great Lakes by volume and encompasses three distinct basins (Georgian Bay, North Channel, and the main basin which includes Saginaw Bay). The physical features of Lake Huron have been described well in a number of previous works (Saylor and Miller 1979; Sheng and Rao 2006; Nguyen et al. 2014). A notable feature of the lake is a mid-lake ridge extending southeastward from Alpena to Point Clark that separates the lake into the southwestern and northeastern basins. The deepest part of the lake, which is north of Alpena, exceeds 230 m in depth. Lake Huron is affected by natural and anthropogenic activities resulting in water quality degradation, invasion of zebra mussels (Fahnenstiel et al. 1995; Heath et al. 1995; Bierman et al. 2005; Fishman et al. 2009), the presence of toxic contaminants, and eutrophication in nearshore areas (Nalepa et al. 2007). Water quality problems including elevated levels of bacteria such as *Escherichia coli* (Alm et al. 2006; Ge et al. 2012), and mercury contamination (Marvin et al. 2004) are also pertinent issues. Shallow areas and embayments such as Saginaw Bay are believed to

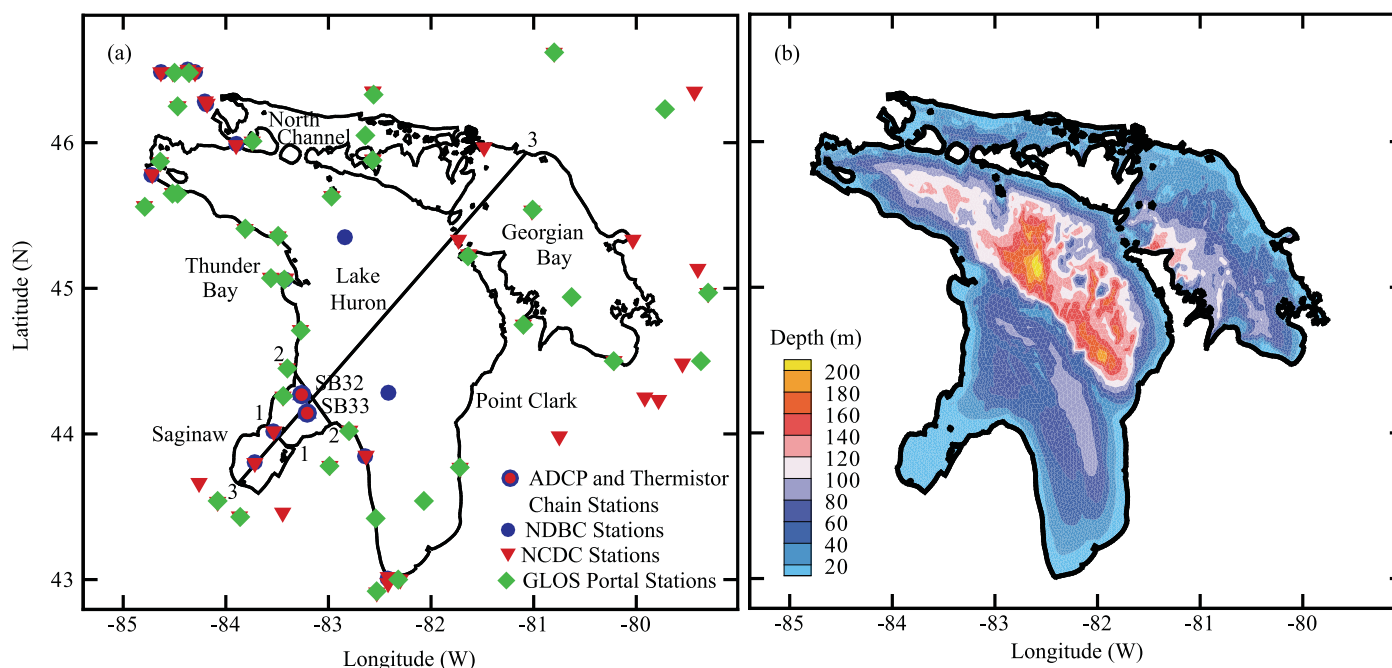


**Fig. 1.** (a) Map of Lake Huron showing the bathymetry and observational stations. 1-1 is the boundary between inner and outer Saginaw Bay. 2-2 is the boundary between outer Saginaw Bay and Lake Huron. The transect 3-3 is used to show vertical variations of temperature in the lake. (b) Bathymetry of Lake Huron. [Color figure can be viewed at [wileyonlinelibrary.com](http://wileyonlinelibrary.com)]

have encouraged increased benthic algal growth from invasive mussels (Hecky et al. 2004). Lake Huron is a connecting waterway between the upper and lower Great Lakes, so contamination will impact not only the Lake Huron ecosystem but also the ecosystems of the lower lakes.

Lake Huron is partially covered with ice during the winter seasons and the ice cover directly affects circulation, thermal structure, mixing and the residence time of pollutants within the lake. The ice cover on Lake Huron (and on the entire Great Lakes) has been declining since 1973. More recently, due to very cold temperatures across North America at the end of April 2014, roughly 23% of Lake Huron was covered by ice (Clites et al. 2014). This is considerably more than is usually present at that time—the 40-yr record shows only a few instances where the ice cover exceeded 10%.

#### Numerical model

We use an unstructured-grid, three-dimensional hydrodynamic model (FVCOM) coupled with a two-dimensional ice model (CICE, Hunke et al. 2013) to understand the nature of circulation and the extent of ice cover over Lake Huron during four winter seasons (2008–2009, 2009–2010, 2012–2013, and 2013–2014) and to quantify exchange rates between Saginaw Bay and Lake Huron. These winters were chosen because in situ observations were available for 2008–2009 and 2009–2010, and they are representative of low ice cover years (2009–2010 and 2012–2013) and high ice cover years (2008–2009 and 2013–2014) in which the winter 2014 was

one of the coldest years on record in the Great Lakes. As a result, the area experienced one of the highest ice covers when the maximum ice cover reached 92.5% in Great Lakes and 96.3% in Lake Huron following the ice data statistics for a 41-yr period 1974–2015. FVCOM has been successfully applied in many previous studies of oceans, lakes and rivers (Shore 2009; Anderson and Phanikumar 2011; Gao et al. 2011; Anderson and Schwab 2013; Bai et al. 2013; Nguyen et al. 2014). Gao et al. (2011) used FVCOM coupled with an ice model to test three idealized cases and to simulate ice concentrations and ice velocities in the Arctic region. Their results for the Arctic region show that the model was able to capture the seasonal variability of the ice concentration, coverage, and drift velocities. The unstructured-grid ICE model (UG-CICE) is fully coupled to the Los Alamos Community Ice Code (CICE, Hunke et al. 2013) and details can be found in Gao et al. (2011) and Chen et al. (2013). Major components of the ice model include the thermodynamics, horizontal advection, and ice physical formation. In this study, we used the computational domain (Supporting Information Fig. S1) from our previous research (Nguyen et al. 2014) to investigate winter circulation and ice cover. The domain has 9611 nodes and 17,619 triangular elements in the horizontal and 21 sigma levels in the vertical. Bathymetry at node locations was obtained by interpolating the 6 arc-second bathymetry data downloaded from the NOAA National Geophysical Data Center, Geophysical Data System (GEODAS)

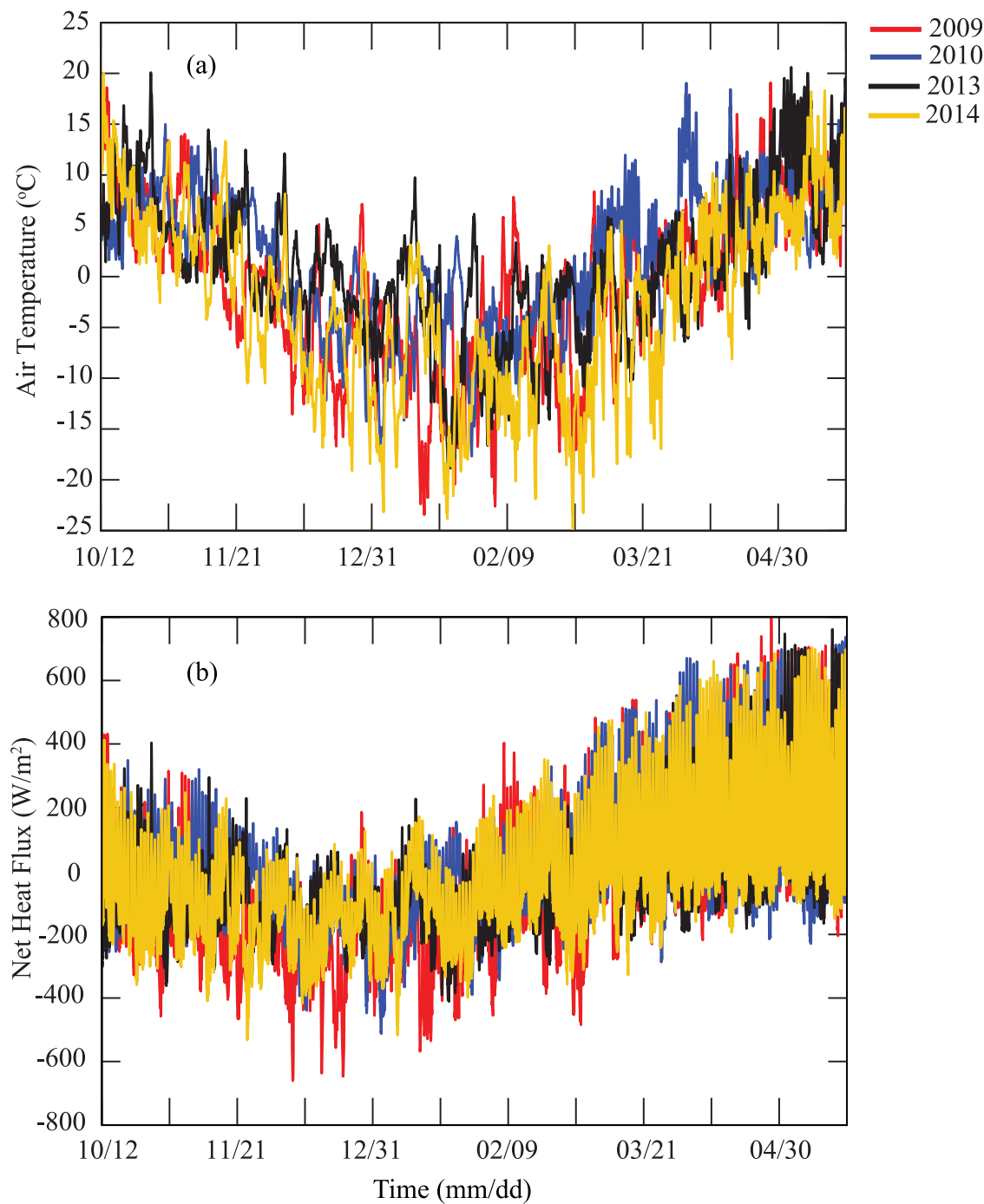


**Fig. 2.** Time series of (a) lake-wide average of air temperature and (b) net heat flux. [Color figure can be viewed at [wileyonlinelibrary.com](http://wileyonlinelibrary.com)]

**Table 1.** Mean values of atmospheric forcing in Lake Huron.

Year	Mean shortwave radiation (W/m <sup>2</sup> )	Mean net heat flux (W/m <sup>2</sup> )	Mean air temperature (°C)
2009	70.3	−105.5	−0.1
2010	60.9	−68.7	−3.3
2013	45.3	−94.1	−4.5
2014	80.5	−86.1	−9.1

**Table 2.** Field measurements, mab is meters above bottom.

Station	Deployed	Retrieved	Longitude	Latitude	Depth (m)	Temperature heights (mab)
SB32	16 Jul 2008	14 Jul 2009	−83.2609°	44.2699°	27.0	1,5,9,13,17,21
SB33	16 Jul 2008	14 Jul 2009	−83.2069°	44.1434°	29.0	1,5,9,13,17,21
SB32	14 Oct 2009	06 May 2010	−83.2609°	44.2699°	27.0	1,5,9,13,17,21,23
SB33	14 Oct 2009	06 May 2010	−83.2069°	44.1434°	29.0	1,5,9,13,17,21,23,25

website (<https://www.ngdc.noaa.gov/mgg/greatlakes/huron.html>). Based on the CFL numerical stability criterion, the external time step used was 3 s and the ratio of internal to external time step was 10. The time step was 30 s for simulating ice transport and thermodynamics. Ice modeling results are sensitive to assumptions about the distribution of ice thicknesses. Hunke et al. (2013) indicate that five categories of ice thickness (the default number of categories used in CICE) are sufficient to simulate the annual cycles of sea ice thicknesses. In Lake Huron all ice is first-year ice and thickness varies from a few cm to a meter or more (Rondy 1976; Fujisaki et al. 2012) with values greater than a meter observed in coastal areas due to the effects of winds and waves. We ran the ice model with different assumptions

about the number of ice categories including 10 categories (as in Fusjisaki et al. 2012), as well as 5 and 2 categories. After carefully examining the sensitivity of model results (Supporting Information Figure S4) and comparing the simulated and observed ice covers and residence times, we have used two categories of ice with thicknesses of 0.5 m and 1.5 m respectively with four sub-layers in each category in addition to the open water category. Parameters used in the ice model and additional details are summarized in Supporting Information Table S1.

The hydrodynamic model contains the primitive equations based on the hydrostatic assumption in the vertical direction with the Boussinesq simplification for convective flows. Ice movement has an important role on lake circulation and

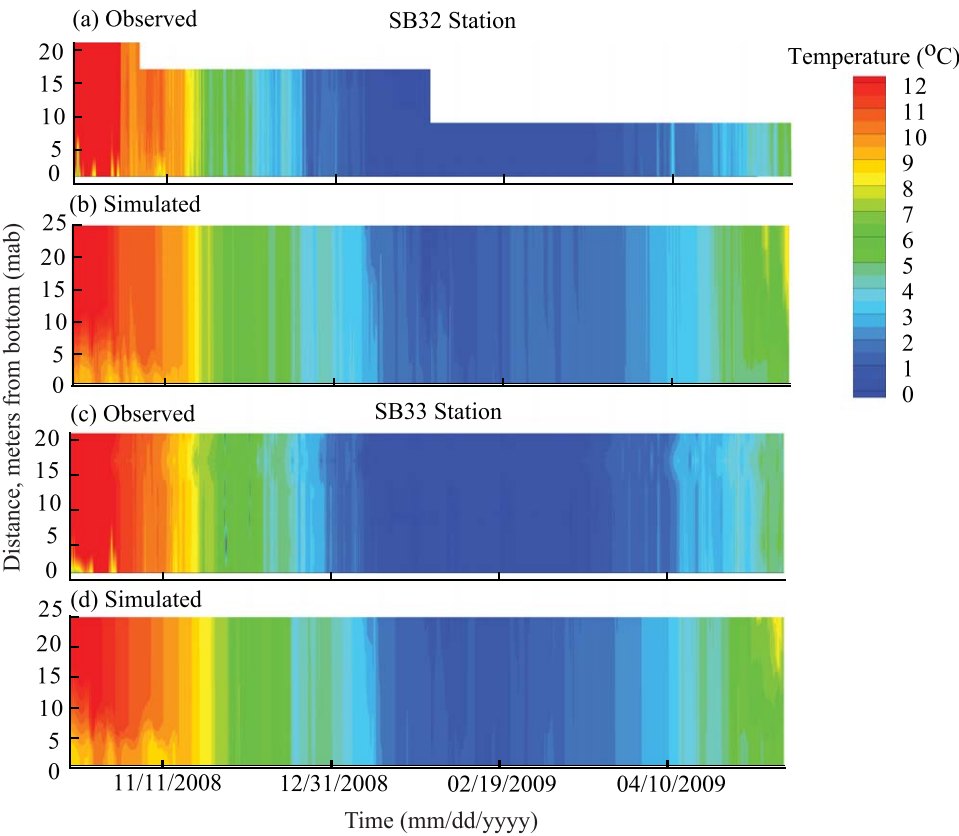


**Fig. 3.** Time series of observed (thermistor chain data) and simulated temperatures in the water column at stations SB32 (a and b), and SB33 (c and d) for winter 2009. [Color figure can be viewed at [wileyonlinelibrary.com](http://wileyonlinelibrary.com)]



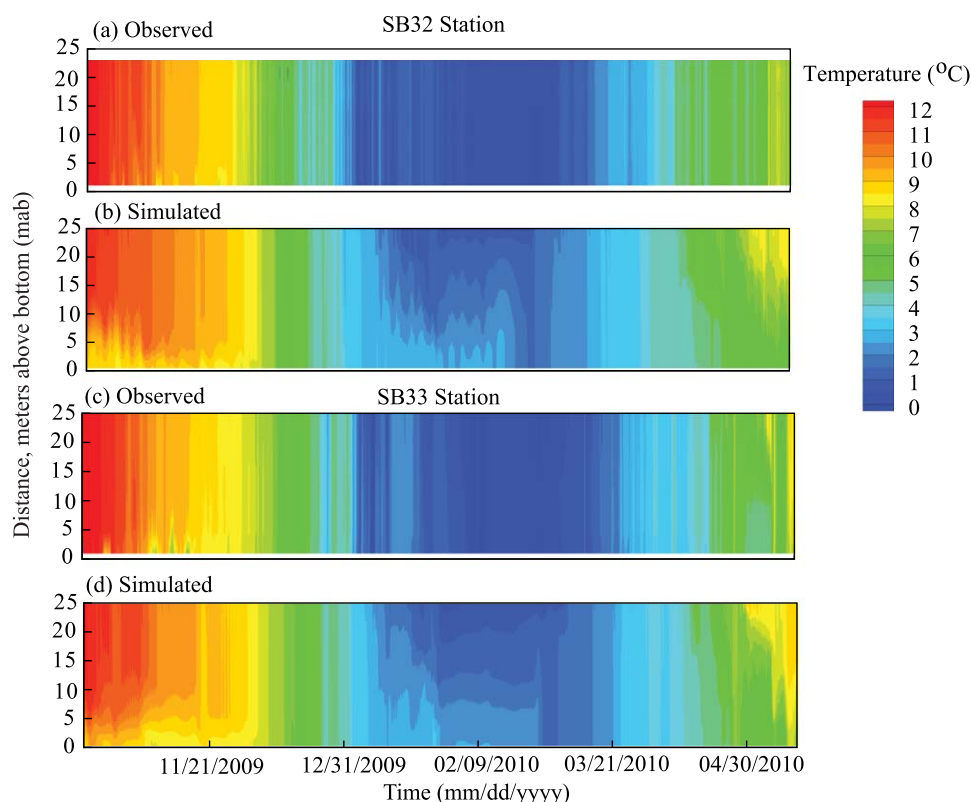


**Fig. 4.** Time series of observed (thermistor chain data) and simulated temperatures in the water column at stations SB32 (**a** and **b**), and SB33 (**c** and **d**) for winter 2010. [Color figure can be viewed at [wileyonlinelibrary.com](http://wileyonlinelibrary.com)]

thermal processes. The drifting of ice, which is influenced by a combination of water movement and wind stress, will lead to a redistribution of water temperature. Details of the governing equations and boundary conditions can be found elsewhere (e.g., Chen et al. 2003, 2013; Hunke et al., 2013).

Winter conditions usually begin in December of the previous year and last until late March to early April in the next year. In order to avoid confusion in the wintertime definition, we use the second year as the year of winter. For the four winters studied in this paper, the hydrodynamic model simulations were started on 06 May 2009 and 10 April in 2008, 2012, and 2013 respectively with zero velocity and uniform vertical temperature profiles to avoid problems with initialization of the stratified temperature. The models ran until end of May in the following years. The initial temperature conditions were set up at 2.5°C for 2009 and 3.5°C for 2008, 2012, and 2013.

#### Meteorological and observational data

As described in Nguyen et al. (2014), wind speed, wind direction, air temperature, relative humidity, and cloud cover fractions for the years 2010, 2013, and 2014 were downloaded from 14 National Data Buoy Center (NDBC) stations (<http://www.ndbc.noaa.gov/>), a large number of which are operated either by the National Weather Service (NWS) or

Environment Canada, and additional data were downloaded from 27 stations on the Great Lakes Observation System (GLOS) portal (<http://glos.us/>). These stations are shown in Fig. 1. The data were interpolated to the computational grids using a smoothed nearest neighbor method (Schwab 1999). Additional details, including the method of calculation of shortwave radiation, sensible heat, and latent heat can be found in Nguyen et al. (2014). For winter 2009, data from a large number of meteorological stations are unavailable from the GLOS portal, therefore we blended the available data with outputs from the Weather Research and Forecasting (WRF) model (Skamarock et al. 2008) to obtain sufficient data for simulating winter 2009. We used the WRF model with a grid spacing of 32 km for the Great Lakes area with a nested grid spacing of 11 km for Lake Huron to dynamically downscale the NCEP Global Final Analysis (FNL). The WRF domain for the research area is shown in the Supporting Information Fig. S2. The meteorological data were then interpolated from WRF grids to the Lake Huron computational grids. This approach (using WRF model to drive FVCOM) has been successfully applied in a number of previous studies (Chen et al. 2012; Nakamura et al. 2015; Yang et al. 2015). Prevailing wind directions in the form of wind rose plots are shown in Supporting Information Fig. S3 for

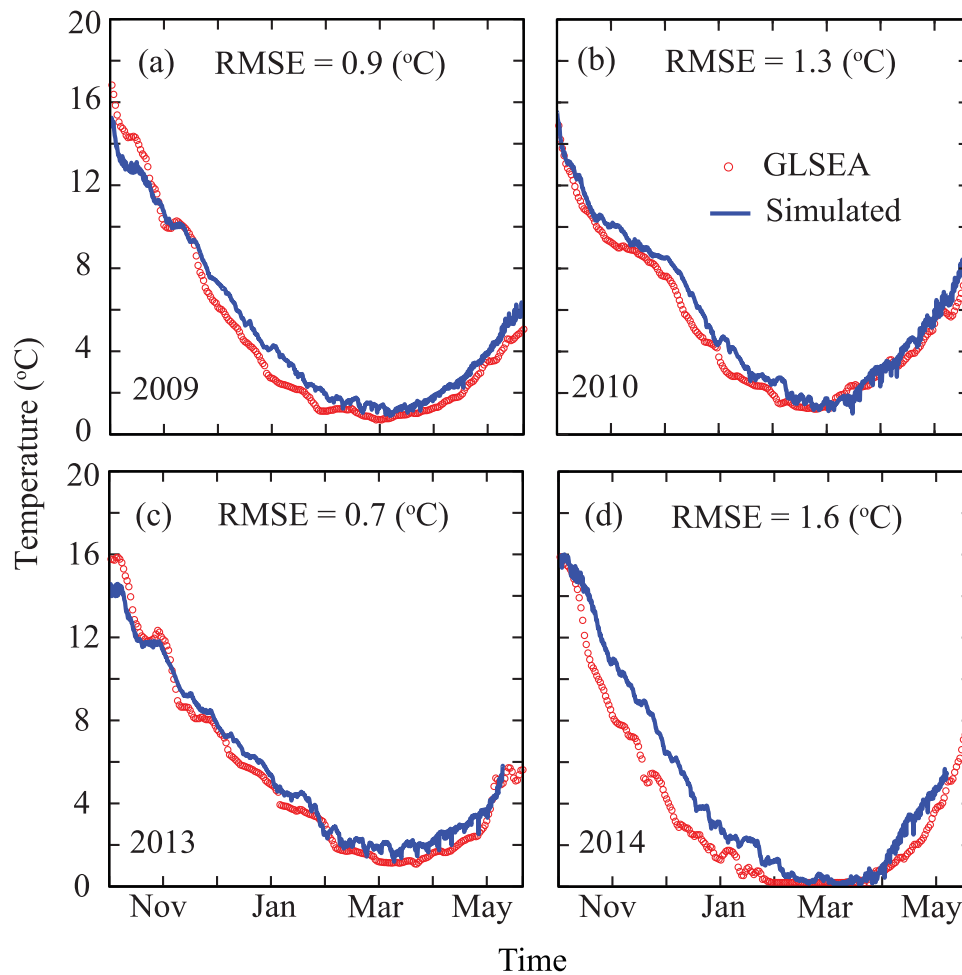


**Fig. 5.** Comparison between lake-wide averaged simulated surface temperatures and observed data processed by GLSEA for (a) winter 2009, (b) winter 2010, (c) winter 2013, and (d) winter 2014. [Color figure can be viewed at [wileyonlinelibrary.com](http://wileyonlinelibrary.com)]

two years. These show that wind conditions varied considerably both from month to month and between the years. The NDBC moorings in the lake are removed each fall and are not redeployed until spring, so no surface water temperatures were measured during the winter. Therefore we used the analysis of surface water temperature from the Great Lakes Surface Environmental Analysis (GLSEA). The GLSEA data provide daily water temperatures derived from NOAA's polar-orbiting satellite imagery obtained through the Great Lakes CoastWatch program. Hourly time series data of air temperature and net heat flux during the winter months for the 4 yr are shown in Fig. 2 and summarized in Table 1. The observed ice concentration data were downloaded from the Great Lakes Ice Atlas (<http://www.glerl.noaa.gov/data/ice/>).

Fieldwork was conducted during the winters of 2009 and 2010. In the winter 2010 two ADCPs (RD Instruments Workhorse Sentinel) were deployed to measure current velocities at the mouth of Saginaw Bay (Fig. 1, stations SB32 and SB33).

Measurements were made in 1-m bins at 20-min intervals. Details of the deployments are listed in Table 2. Time series measurements of water temperature during winter 2009 and 2010 were also collected at SB32 and SB33 with chains of Onset Tidbit and Seabird SB39 temperature recorders. These sensors recorded point measurement every hour. Sensor heights in meters above bottom (mab) are also given in Table 2. Additional information is given in Hawley et al. (2014).

## Results

### Temperature

Observations of water temperature at the thermistor chain stations SB32 and SB33 near the mouth of Saginaw Bay are shown in Fig. 3 (winter 2009) and Fig. 4 (winter 2010). The simulated temperature was calculated at 21  $\sigma$ -levels through the water column rather than the seven observational levels at station SB32 and 10 levels at station SB33. The blank area at SB32 station measured in winter 2009 (Fig. 3a) indicate the missing data due to sensor errors. Although the model

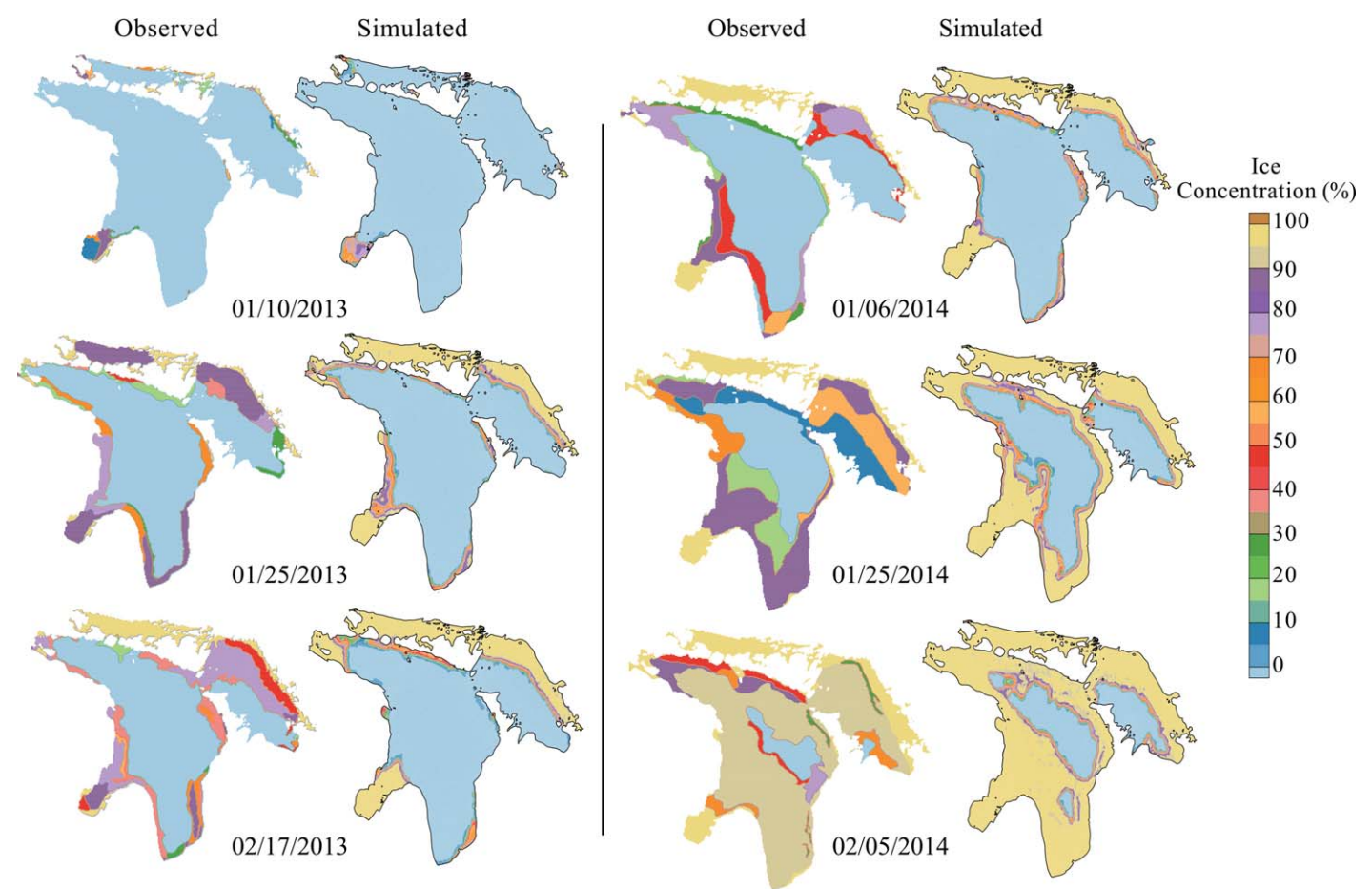


**Fig. 6.** Map of Lake Huron showing observed and simulated ice cover area for winters 2013 and 2014. [Color figure can be viewed at wileyonlinelibrary.com]

**Table 3.** Maximum ice cover in Lake Huron (%)

Year	Simulated	Observed
2009	63.6	85.3
2010	32.7	38.7
2013	32.8	45.6
2014	97.8	96.3

does not accurately simulate either the breakdown of the thermocline in the fall, or its formation in the spring, the results are in good overall agreement with the observations during the period of ice cover (January–March) with simulated water temperatures being warmer longer compared to observations. Simulated water temperatures were also compared to lake-wide averaged surface temperature (GLSEA) derived from NOAA polar-orbiting satellite imagery (Fig. 5). These show good agreement with the observations with RMSE values ranging from 0.7°C to 1.6°C.

**Ice cover, ice concentration, and ice thickness**

The comparisons between simulated and observed ice cover are shown in Fig. 6 and Table 3. The simulated percentage

of ice cover over Lake Huron is calculated as a product of grid area and ice concentration over a total area of  $5.88 \times 10^4 \text{ km}^2$ . Although we calculated ice cover extent over Lake Huron for 4 yr, only the spatial map results for 2013 and 2014 are shown. This is because of differences in the way ice cover data are processed and displayed for year 2009 and 2010 for which a band of constant ice concentration was used all around the lake. The distributions of observed ice concentration are reasonably well represented by the ice model. Because over-lake precipitation and evaporation were not included in the mass balance of the ice model (latent heat is accounted for in the heat balance), differences between observed and simulated ice cover can be expected. Most of the ice cover in the lake occurred in Saginaw Bay, North Channel, and Georgian Bay during January and February while there were large areas of open water during both winters. Figure 7 shows the time series of simulated ice cover compared to the observations for the four years. The results show that the ice model simulated the extent of ice cover well in years with low ice cover. The RMSE values for the two low ice cover years are 5.8% and 5.0% for the winters of 2010 and 2013 respectively while the corresponding



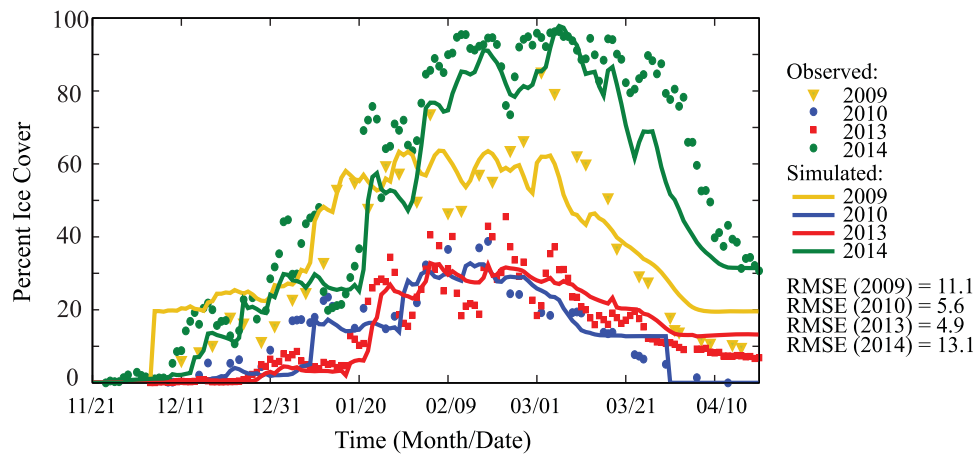


**Fig. 7.** Time series of observed and simulated percent ice cover over Lake Huron during the winters of 2009, 2010, 2013, and 2014. [Color figure can be viewed at [wileyonlinelibrary.com](http://wileyonlinelibrary.com)]

**Table 4.** Monthly mean and maximum simulated ice thickness (cm) in Lake Huron and Saginaw Bay.

Year	Area	January		February		March	
		Mean	Max	Mean	Max	Mean	Max
2009	Lake Huron	3.7	67.8	7.7	98.4	6.6	78.5
	Saginaw Bay	8.1	51.5	17.4	52.9	8.0	53.3
2010	Lake Huron	1.7	60.0	4.8	53.5	1.2	36.0
	Saginaw Bay	4.5	21.7	11.5	22.5	2.7	22.4
2013	Lake Huron	1.5	42.2	6.2	95.4	5.0	40.0
	Saginaw Bay	3.7	30.4	11.8	23.4	8.8	35.4
2014	Lake Huron	9.0	124.7	19.5	130.6	20.5	148.1
	Saginaw Bay	24.5	51.3	30.5	50.3	28.9	39.0

numbers for the two high ice cover years are 11.1% and 13.1% for the winters of 2009 and 2014 respectively. These comparisons between observed and simulated ice cover are similar to those reported in the literature in recent years e.g., (Fujisaki et al. 2013).

High resolution (250 m) satellite images of Saginaw Bay from NASA's Earth Observatory (<https://earthdata.nasa.gov/labs/worldview/>) were used to compare with the ice cover area results from our ice modeling. Based on the available data on cloud-free days we selected images from several days during winters 2013 and 2014. The comparisons between simulated and observed ice cover areas are shown in Supporting Information Fig. S5. Saginaw Bay is almost entirely ice covered during the winter especially in the inner bay area where the maximum ice concentrations reach 100%. Supporting Information Figure S6 shows the comparison between simulated and observed ice cover on 09 March 2014 when the lake is fully covered by ice.

Mean ice thickness over the 3 months of winter for the 4 yr was 7.2 cm for Lake Huron and 13.4 cm for Saginaw Bay.

Summary statistics for the simulated ice thicknesses in winter months for Lake Huron and Saginaw Bay are presented in Table 4 for the four simulated years. The maximum ice thickness was reached in March, 2014 with a value of 148 cm for Lake Huron (the maximum ice thickness in Lake Huron usually occurs in the North Channel). In Saginaw Bay, the maximum ice thickness value was 53.3 cm in March 2009.

### Circulation

A comparison of observed and simulated vertically integrated currents at stations SB32 and SB33 is shown in Fig. 8. Values of the mean and maximum currents for different winter months are provided in Table 5 and summary statistics for the comparisons in Fig. 8 are provided in Table 6. Ice formation start and end dates at the ADCP locations are marked in Fig. 8 using dashed lines. Spatial patterns of circulation within the Saginaw Bay and the entire lake are shown in Fig. 9 and Supporting Information Fig. S7 respectively as vertically integrated velocities averaged over the winter months of January, February, and March. The dominant current patterns are marked using thick red lines with arrows showing the direction of flow.

### Flushing and residence times

The high concentration of ice in Saginaw Bay significantly impacts the flushing rates both between the outer and inner bays (transect 1-1 in Fig. 1) and between the outer bay and the open lake (transect 2-2). We used the same approach and definitions of residence time and flushing time as in our previous work (Nguyen et al. 2014) and calculated the water exchange rates and flushing times for the bay for the winters of 2009, 2010, 2013, and 2014. Briefly, the flushing time is defined (see, for example, Monsen et al. 2002) as the ratio of the volume ( $V$ ) of the bay to the rate of inflow  $Q$  (or outflow, since this is a steady-state concept):

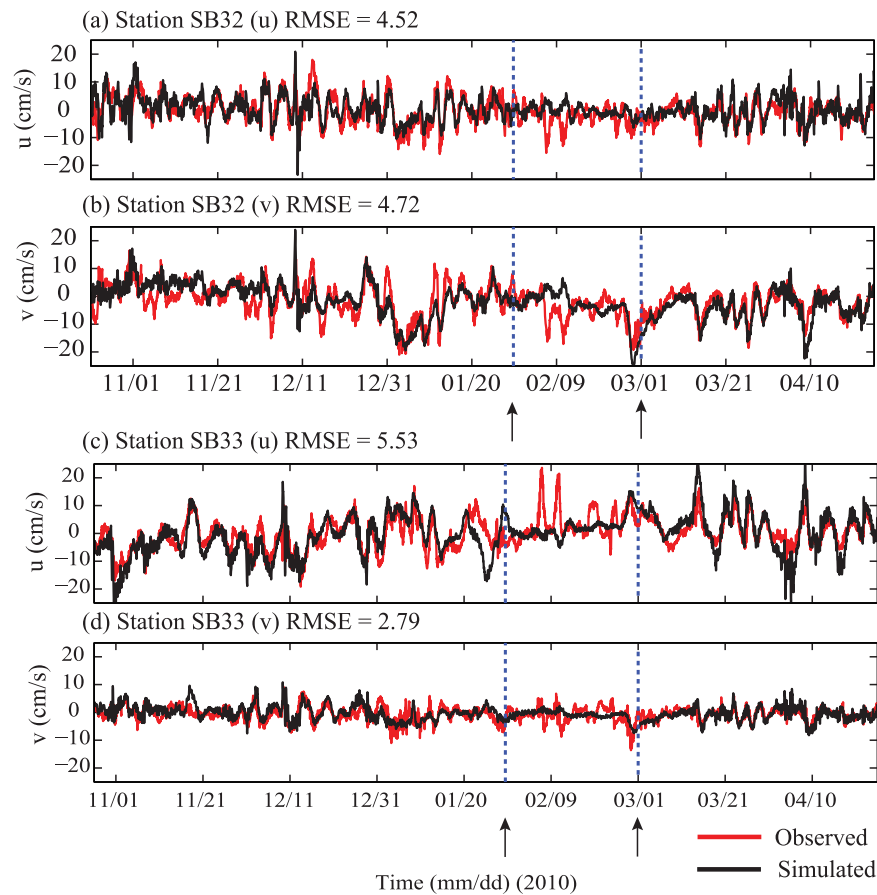


**Fig. 8.** Comparison of observed and simulated vertically-averaged velocities at locations SB32 (a and b) and SB33 (c and d). Blue dashed lines (and the arrows) indicate the starting (30 January 2010) and ending (01 March 2010) dates of ice formation at the ADCP locations. [Color figure can be viewed at [wileyonlinelibrary.com](http://wileyonlinelibrary.com)]

**Table 5.** Mean and maximum vertically averaged currents in Lake Huron (cm/s).

Year	December		January		February		March	
	Mean	Max	Mean	Max	Mean	Max	Mean	Max
2009	2.4	23.3	0.8	9.9	0.2	2.5	0.2	2.1
2010	1.2	12.0	1.6	9.7	1.4	15.0	1.3	8.3
2013	0.72	4.5	1.4	10.5	0.6	4.9	1.0	7.4
2014	0.8	5.8	0.76	6.5	0.34	3.4	0.3	2.9

**Table 6.** Comparisons of observed and simulated velocity (cm/s).

Station	Components	Mean		Standard deviation		RMSE
		Observed	Simulated	Observed	Simulated	
SB32	East	−0.6	0.01	4.7	4.5	4.5
	North	−1.9	−2.0	5.7	6.0	4.7
SB33	East	0.3	0.2	5.7	7.6	5.5
	North	−0.6	−0.4	2.7	2.7	2.8

$$T_i = \frac{V}{Q} \tag{1}$$

Since the vertically integrated current velocities in winter in Saginaw Bay area were lower than in summer, the flushing times can be expected to be longer than the corresponding values in summer. The simulated vertically averaged volumetric inflow  $Q$  as a function of time is presented in Fig. 10 for transects 1-1 and 2-2 (shown in Fig. 1) respectively. The complexity of the exchange rates at the inner transect during wintertime can be seen from the fluctuations of the volumetric influx and the variations in the magnitude of the

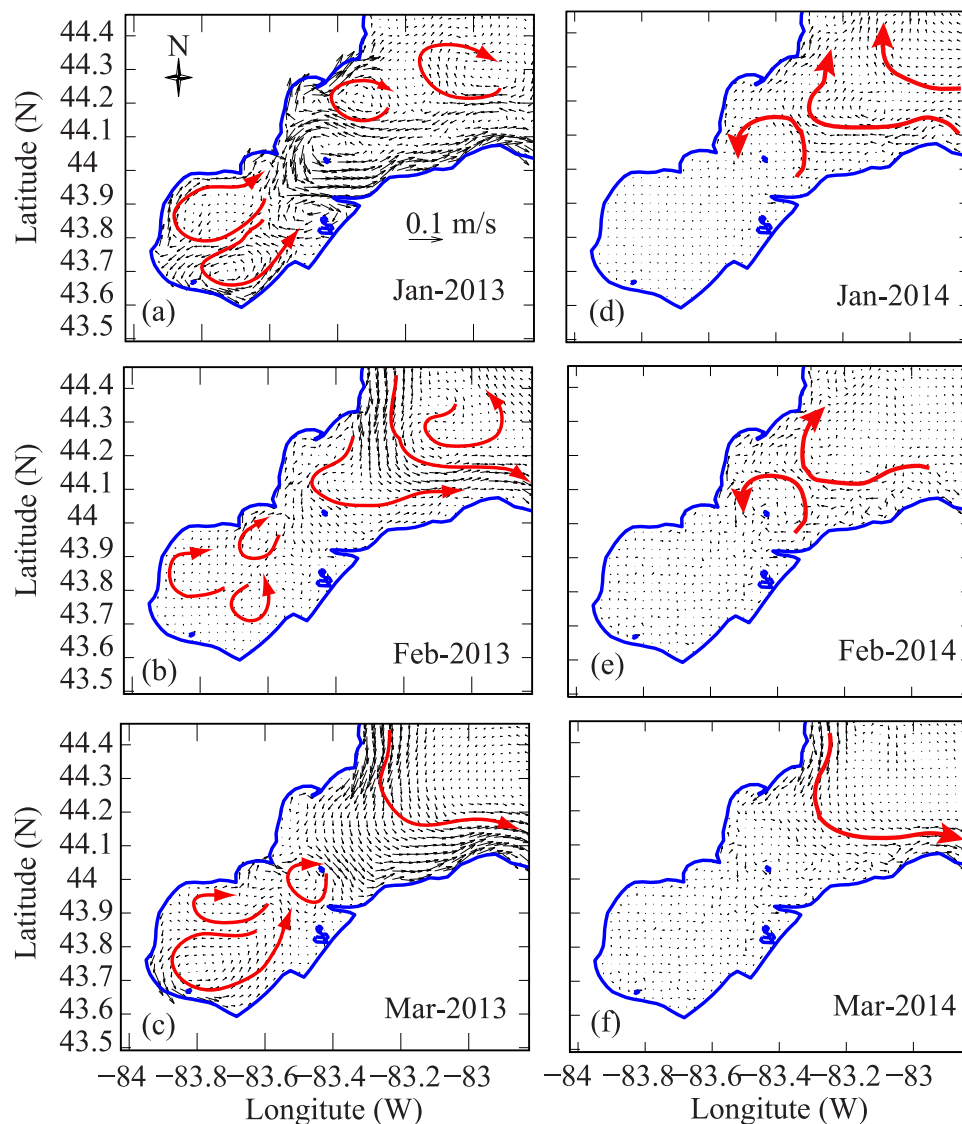


**Fig. 9.** Mean (vertically averaged) monthly currents in Saginaw Bay during the winter months of years 2013 (**a,b** and **c**) and 2014 (**d,e**, and **f**). The dominant current patterns are marked using thick red lines with arrows showing the direction of flow. [Color figure can be viewed at [wileyonlinelibrary.com](http://wileyonlinelibrary.com)]

fluctuations between the two winters. We notice that volumetric inflow (water exchange) during winter 2014 with high ice cover decreased by two orders of magnitude at the outer transect 2-2 relative to the values in 2009. Comparison with similar exchange rates for summer months reported in (Nguyen et al. 2014, Fig. 19) indicates that water exchange rates at the outer transect 2-2 during winter months show significantly larger variability—a variation of over six orders of magnitude in winter compared to one order of magnitude variation during the summer months. Flushing times computed based on Eq. (1) and the monthly average flow rates  $Q$  in Fig. 10 are summarized in Table 7.

There are many definitions of residence time in the literature as described in Nguyen et al. (2014). In the present paper,

the residence times are computed and expressed as e-folding flushing times for the inner and the entire Saginaw Bay. They were calculated for two cases—with and without using the ice model for low and high ice cover years. The bay was treated as a CSTR (continuously stirred tank reactor; Chapra 2008) and a tracer was released instantaneously at an initial concentration of  $C_0 = 100$  ppm in every grid cell in the bay area. The residence time is the time required for each element's vertically integrated concentration to fall below  $1/e$  of its initial vertically integrated concentration (Burwell et al. 2000). Since this definition provides a local measure with one value of residence time for every grid cell, a measure of residence time for the entire bay was obtained by averaging the vertically integrated concentrations for all grid cells. The time for this average vertically-

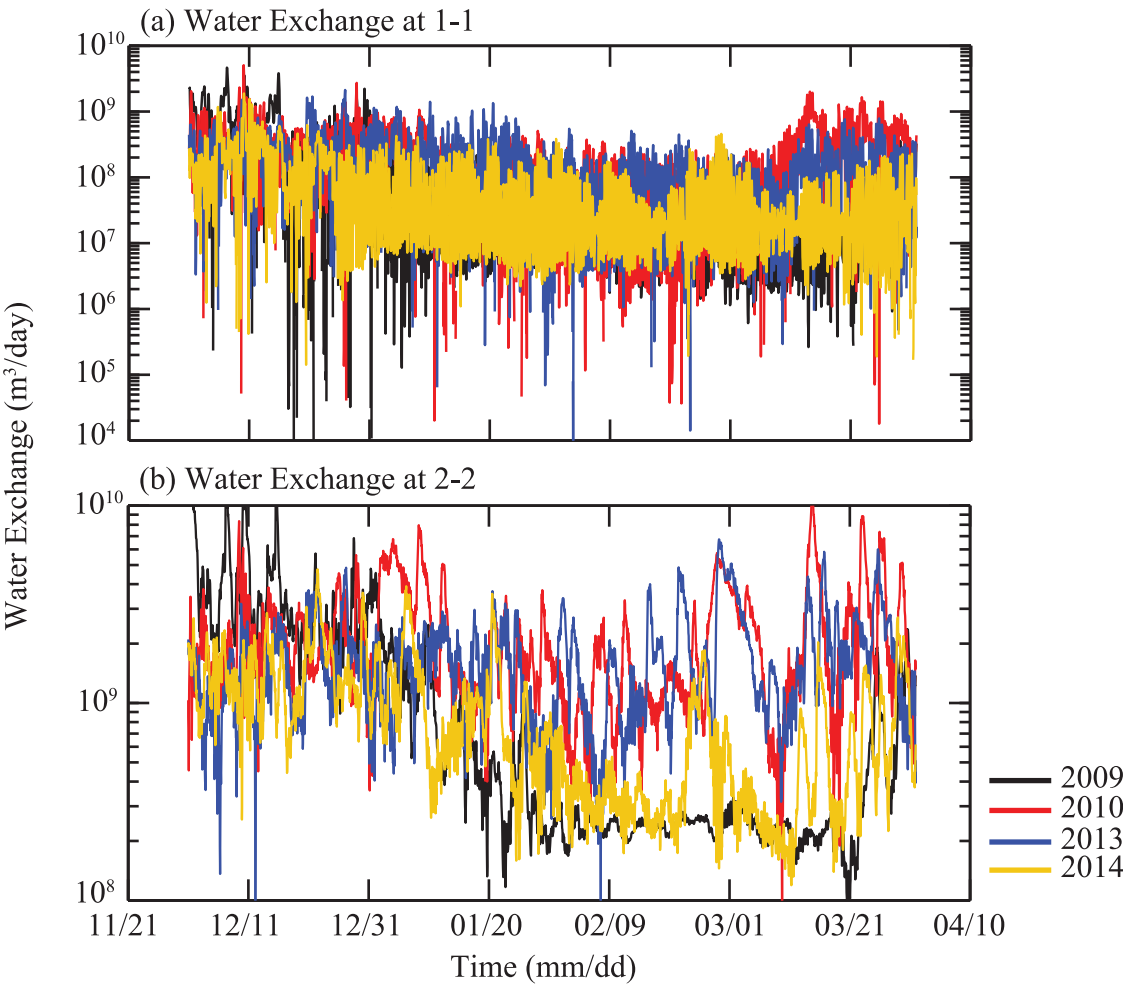


**Fig. 10.** Time series of water exchange rates (a) between inner and outer Saginaw Bay (at transect 1-1 in Fig. 1) and (b) between the outer bay and Lake Huron (at transect 2-2 in Fig. 1) in Saginaw Bay in winter season. [Color figure can be viewed at [wileyonlinelibrary.com](#)]

**Table 7.** Mean flushing time (days) for inner Saginaw Bay and for the entire bay.

Year	Area	December	January	February	March
2009	Inner bay	10.9	109.7	154.2	197.3
	Entire bay	7.8	34.8	124.4	69.4
2010	Inner bay	15.2	33.9	108.0	18.1
	Entire bay	13.9	11.7	18.5	11.2
2013	Inner bay	20.8	27.0	75.7	46.9
	Entire bay	18.8	19.7	16.6	14.5
2014	Inner bay	31.3	96.7	147	176
	Entire bay	19.9	29.5	64.8	49.9

integrated concentration ( $\bar{C}$ ) to fall below  $(1/e)$  of its initial value then provides an integrative measure of residence time for the entire bay and is denoted as  $\bar{\tau}_R$ . We use the Saginaw river discharge measured at USGS station 04157005 as inflow to the hydrodynamic model but it had zero tracer concentration.

In order to understand how residence time values change under low and high ice cover conditions, we model tracer transport and compute residence times for two recent winters—2013 (low ice cover year) and 2014 (high ice cover year). Residence time results for the inner bay and the entire bay are presented in Fig. 11 for 2013 and 2014 in the form of contour plots. Although one definition of winter includes only the period from 21 December to 20 March (from winter solstice to the vernal equinox), cooling of air (and hence lake water) starts much earlier and gradual warming continues with time. For both years, the dye concentration model was run continuously from 20 November of the previous year to the end of May of the following year—longer than the winter period according to the above definition. The dye was released with the hydrodynamic conditions fully established in the bay. The results show the important role played by the gyres since there was an area with lower residence times near the mouth of Saginaw Bay in both cases. For 2013, the mean residence times are 65.1 d (2.2 months) and



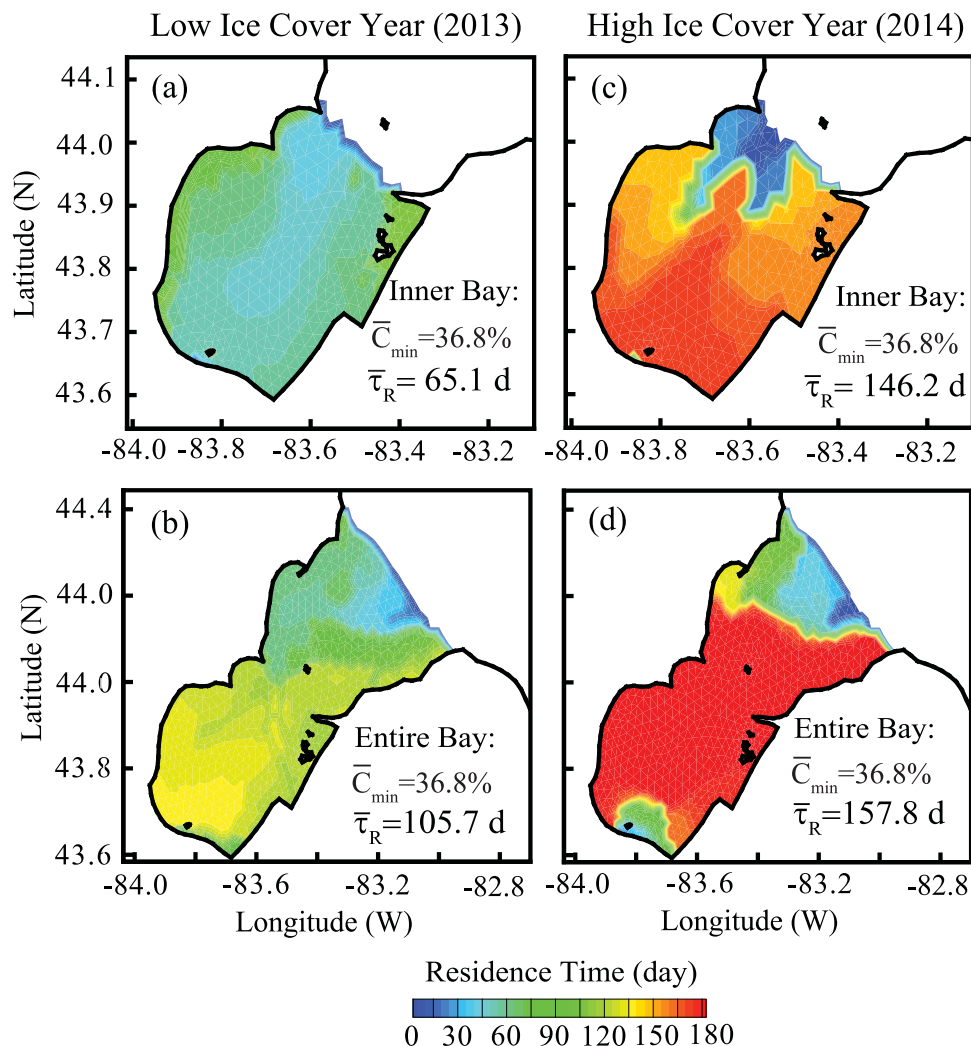


**Fig. 11.** Contour plots of residence time for Saginaw Bay based on dye concentration modeling. (a and b) are for the inner bay and the entire bay under low ice cover. (c and d) are for the inner bay and the entire bay for a high ice cover year. [Color figure can be viewed at [wileyonlinelibrary.com](http://wileyonlinelibrary.com)]

105.7 d (3.5 months) for the inner bay and the entire bay respectively. With high ice cover (2014) the corresponding numbers are 146.2 d (4.9 months) and 157.8 d (5.3 months), respectively. To understand how ice cover influences residence times, we simulated a hypothetical case in which winter meteorological forcing was used to run the models but the ice model was not used. The mean residence times estimated for the inner and outer bays for this scenario without ice cover are 64.7 d and 114.2 d, respectively. These estimates are not significantly different from those for the summer months, where the mean residence times for the two areas are 62 d and 115 d, respectively (Nguyen et al. 2014). This implies that for the winter season with less ice formation the mean residence times approach the corresponding values for the summer months. While circulation patterns can be expected to change quickly due to warming in late spring and early summer resulting in increased flushing

rates, these results essentially indicate that the dye was stored in the bay throughout the winter months when considering the entire Saginaw Bay.

## Discussion

### Thermal structure

Similar to the other Laurentian Great lakes, Lake Huron is dimictic and experiences fall and spring overturns between which periods of relatively homogeneous conditions prevail. This important feature has been reproduced in the model although the timing is somewhat off. At the end of fall (mid-November) the lake is almost homogenous in temperature both vertically and horizontally with a water temperature of around 8°C (Figs. 3, 4). As cooling of air continues in late fall, the water temperatures decrease starting in shallow areas such as the inner Saginaw Bay, Georgian Bay and some

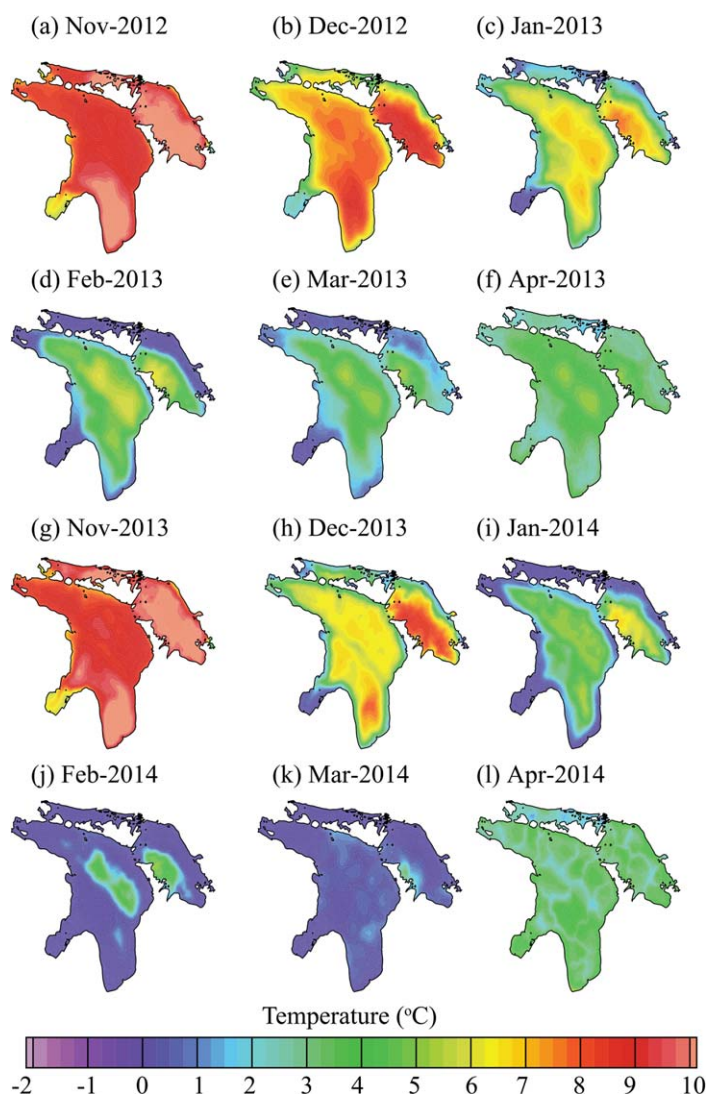


**Fig. 12.** Surface temperature contours in Lake Huron for the winter months in years 2013 (a,b,c,d,e,f) and 2014 (g,h,i,j,k,l). [Color figure can be viewed at [wileyonlinelibrary.com](http://wileyonlinelibrary.com)]

areas in the Northern Bay. Rapid cooling in the nearshore areas occurred in January and February. During these 2 months the horizontal temperature gradient between the nearshore areas and mid-lake region reached 5°C, which is larger than the 3°C gradient observed by Saylor and Miller (1976). In March, Lake Huron is almost homogeneous at a temperature of 3°C. The transition of thermal structure from winter to spring conditions is also supported by the observed and simulated vertical temperature profiles presented in Figs. 3, 4 where the lake is almost entirely homogeneous in temperature by mid-November.

The lake-wide average of temperatures at surface, mid-depth, and bottom through the winter and spring months show some differences (for example, see Supporting Information Fig. S8 for two representative years). Fall temperatures were isothermal and cooled from about 7–4°C during

December in 2009, and from late November until mid-January in 2012–2013. The effects of the colder winter in 2013 are apparent in the delayed formation of the thermocline that year (beginning in May in 2013 vs. mid-April in 2010). Monthly averaged surface temperatures for different winter months are shown in Fig. 12 for one low ice (2013) and one high ice (2014) years. The vertical variations in temperature along the transect 3-3 (in Fig. 1) are shown in Fig. 13. Following a period of relatively uniform temperature in the lake during the month of December, the months of January, February, and March are characterized by faint horizontal gradients in temperature in the deeper portions of the lake with ice or relatively cold water in the bays and other shallow areas. These observations are consistent with the conclusions of Saylor and Miller (1979).

The monthly average surface temperature maps for Saginaw Bay (Supporting Information Fig. S9) clearly show that the bay was essentially isothermal by November and that it remained so until April. There is a well-defined “thermal boundary” located near the inner transect 1-1 in December when the difference in temperature between the inner bay and outer bay was about 2.5–3.0°C. As the air temperature continued to decrease, the thermal boundary moved lakeward until the entire bay became homogeneous. The presence of this thermal boundary temperature is associated with the bathymetric features in the bay. Since the mean depth in the inner bay is about 4 m, the water temperature decreased relatively quickly compared to the outer bay where the mean depth is approximately 8 m.

### Ice cover

To better understand how atmospheric forcing influences ice cover extent and circulation, we examine the lake-wide averages of air temperature, shortwave radiation, and net heat flux shown in Fig. 2 and Table 1. The mean values of shortwave radiation over wintertime for the years 2009, 2010, 2013, and 2014 are 70.3 W/m<sup>2</sup>, 60.9 W/m<sup>2</sup>, 45.29 W/m<sup>2</sup>, and 80.5 W/m<sup>2</sup>, respectively. The range of the mean net heat flux during winter over 4 yr are from –105.5 W/m<sup>2</sup> to –68.7 W/m<sup>2</sup> in which the minimum value was reached in winter 2009. The modeled ice covers show that in winter 2009 the date for the onset of ice was 05 December 2008 and the ice cover persisted until 12 May 2009. The corresponding dates for winters 2010, 2013, and 2014 are (12/07/2009 to 03/30/2010), (11/8/2012 to 04/26/2013), and (11/24/2013 to 5/23/2014), respectively. The winter of 2014 had the longest period of ice formation (180 d) while the winter of 2010 had the shortest period of time with ice cover (113 d). As shown in Figs. 2 and 7, ice cover increased rapidly starting on (01/18/2009), (01/10/2010), (01/23/2013), and (01/20/2014) after the net heat flux reached its minimum value in these years: –568 W/m<sup>2</sup> on 01/14/2009, –508 W/m<sup>2</sup> on 01/02/2010, –396 W/m<sup>2</sup> on 01/22/2013, and –517 W/m<sup>2</sup> on 01/07/2014. The maximum values of ice cover were 63.6%, 32.7%, 32.8%, and 97.8% when the lake-wide mean air

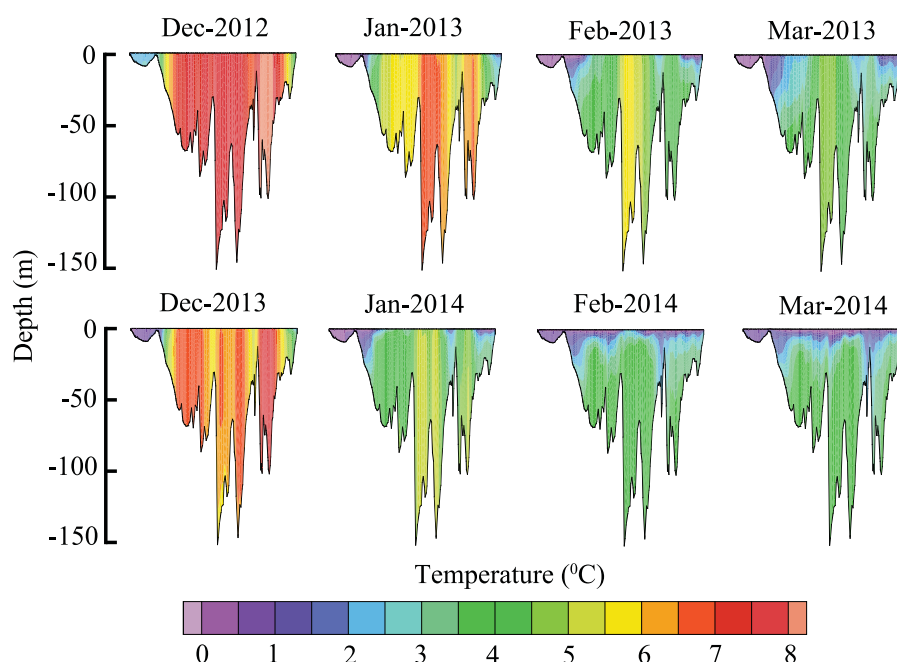


**Fig. 13.** Vertical variations of temperature in Lake Huron for winters of 2013 and 2014 along the transect 3-3 in Fig. 1. [Color figure can be viewed at [wileyonlinelibrary.com](http://wileyonlinelibrary.com)]

temperatures were  $-0.1^{\circ}\text{C}$ ,  $-3.3^{\circ}\text{C}$ ,  $-4.5^{\circ}\text{C}$ , and  $-9.1^{\circ}\text{C}$  in 2009, 2010, 2013, and 2014, respectively. Summary statistics of maximum values of simulated and observed ice areas are shown in Table 3.

As shown in Fig. 7 and Table 3, model results have generally underestimated the fractional ice cover. The absence of precipitation (especially snow) in the model could be one reason why the model produced less ice growth and this was also noted by Fujisaki et al. (2013). Comparisons between observed and simulated ice cover for Saginaw Bay area are shown in Supporting Information Figs. S5 and S6. The images show ice cover while the panels showing model results show both ice cover and ice concentration. Overall, reasonable agreement between observed and simulated ice cover was noted. Although there were no observations of ice thickness during our study period, simulated ice thickness results for years 2013 and 2014 are shown in Supporting Information Fig. S10. The high ice thickness results for 2014 correlate well with low surface temperatures in the lake (Fig. 12).

### Circulation

During the winter season, large-scale circulation in Lake Huron is influenced by a combination of key physical features (islands, exchange with Saginaw Bay and Georgian Bays, and the mid-lake Alpena-Amberley ridge) and the movement of ice. In the presence of ice, the model results show that winter circulation in the main lake is counter-clockwise (Supporting Information Fig. S3) with a mean

current speed of  $1.0\text{ cm/s}$  (averaged over the three winter months for 4 yr). This result is similar to that reported by Saylor and Miller (1979) who reported a strong cyclonic circulation in the main body of the lake. The complexity of circulation in Saginaw Bay can be seen in Fig. 9, which shows the results of vertically averaged currents for the winter months. Characteristic features of circulation in Saginaw Bay include the presence of a cyclonic gyre at the mouth of the bay and two recirculating cells within the inner bay. The role of ice cover on current velocities can be clearly seen in the presence of stagnant/low current velocity areas associated with ice cover in the inner bay. This can be clearly seen in February when the predominant wind direction over Lake Huron is southeasterly (Supporting Information Fig. S3). To quantify the reduction in the magnitude of currents within the Saginaw Bay due to ice cover, we ran models with and without ice cover and computed the percent reduction in vertically integrated currents in the bay. The % reductions for all grid cells within the bay were then averaged to produce a single number for the entire bay. For February 2010, for example, an average reduction of 71% was estimated over Saginaw Bay due to the presence of ice cover. Fujisaki et al. (2012) also concluded that the packed ice cover slowed down water velocities. The occurrence of stagnant areas due to ice formation imply that the flushing time in winter can be expected to be longer than the flushing time in summer for the inner bay. The reduction of current velocities in winter also implies lower mixing rates in Saginaw Bay. The low



velocity areas in Saginaw Bay disappeared when ice started melting in March for a low ice year (Fig. 9c). Another important feature of circulation during the wintertime is a narrow band of flow about 2 km wide along the mid-lake ridge from Thunder Bay at Alpena across to Point Clark (Supporting Information Fig. S7).

The simulated mean vertical velocity profiles at the inlet of Georgian Bay are illustrated in Supporting Information Fig. S11, where positive and negative values indicate inflow and outflow currents to and from the bay. The results show that there is an outflow at the surface associated with the inflow at the bottom at the mouth of Georgian Bay. This is opposite to the pattern reported by Beletsky et al. (1999) and Nguyen et al. (2014) for the summer months. This difference can be explained by the coupling of homogeneous temperatures with the dominant southeast wind directions in February and March.

### Flushing and residence times

While the flushing time for inner Saginaw Bay is nearly twice as much for the entire bay during summer months (Nguyen et al. 2014), the flushing time is almost similar for the inner and the entire bays in December (Table 7). As the cooling of air continued and with the presence of ice in January, February, and March there was a significant difference in the flushing times between the inner bay and the entire bay. The maximum value of flushing time for the inner bay reached 197 d in 2009. The mean flushing time for the four winters was 57.2 d for the inner bay and 32.8 d for the entire bay. These numbers are significantly greater than the values during the summer months when the corresponding numbers are 23.0 d and 9.9 d, respectively (Nguyen et al. 2014).

The estimated residence times show the important role of ice cover on transport and mixing processes (Fig. 11). The significant change in residence time (e-folding flushing time) with and without ice cover in Saginaw Bay can be explained by the absence of circulation in the bay during the winter months. The stagnant conditions in the bay lead to lower mixing rates although mixing is indirectly influenced by wind through the movement of ice. This implies that in the presence of ice cover, wind stress may not be the predominant factor influencing the residence time, especially in shallow areas such as Saginaw Bay, where the maximum ice thickness was 53.3 cm. The residence time estimates for 2013 indicate that the dye was stored for nearly 2.2 months in the inner bay and for 3.5 months (i.e., over the winter) while considering the entire Saginaw Bay. The estimates for the high ice cover year (2014) are 4.9 months (inner bay) and 5.3 months (entire bay) respectively. The implication of these results is that if contaminants or products of late summer algal blooms are stored in the bay under winter conditions, they can be expected to come out of the inner bay anywhere between late January (low ice cover) and April (high ice cover). Considering the entire bay, the products of

the previous blooms can be expected to be released into the lake between March (low ice cover) and April (high ice cover). Although we computed residence times for only two (one high and one low ice cover) years, these estimates provide upper and lower bounds to residence times under winter conditions and are expected to help in understanding the behavior of contaminants, nutrients and algal blooms in the Saginaw Bay—Lake Huron system.

### Conclusions

An unstructured grid hydrodynamic model coupled with an ice model was used to investigate large-scale circulation, thermal structure, ice cover and exchange in the Lake Huron—Saginaw Bay system. Simulations were conducted for two low (2010 and 2013) and two high (2009 and 2014) ice years respectively. Model results were compared with observed data on currents, water temperatures, and ice cover during the winter months. The model successfully simulated the almost isothermal conditions that occurred during the winter months, and the important features of fall and spring overturn were also reproduced well. The modeled mean ice thickness over the 3 months of winter for the 4 yr was 7.2 cm for Lake Huron and 13.4 cm for Saginaw Bay. As expected, model results show the significant role played by ice cover on lake circulation in winter. Mean circulation in winter was predominantly cyclonic in the main body of Lake Huron with current speeds being highest in January. The mean current speed in Lake Huron was 1.0 cm/s compared to the summer time average of 3 cm/s (Nguyen et al. 2014). The circulation in inner Saginaw Bay was almost stagnant during the period of ice cover. As a result the mean flushing times of the bay are higher than the corresponding flushing times during the summer. Velocity profiles at the mouth of the Georgian Bay during winter were reversed compared to summer conditions with outflow at the surface and inflow at the bottom. Major differences in the residence times of water in Saginaw Bay between summer and winter conditions are found to be due to the effects of ice cover in slowing water velocities in the bay. Considering the entire bay, the residence time estimates for the low (2013) and high (2014) ice cover years indicate that contaminants (or remnants of the previous blooms) entering the bay in late summer can be expected to be released into the lake between March (low ice cover) and April (high ice cover).

### References

- Alm, E., W. J. Burke, and E. Hagan. 2006. Persistence and potential growth of the fecal indicator bacteria, *Escherichia coli*, in shoreline sand at Lake Huron. *J. Great Lakes Res.* **32**: 401–405. doi:10.3394/0380-1330(2006)32[401:PAPGOT]2.0.CO;2
- Anderson, E. J., and M. S. Phanikumar. 2011. Surface storage dynamics in large rivers: Comparing three-dimensional particle transport, one-dimensional fractional derivative



- and multi - rate transient storage models. *Water Resour. Res.* **47**: W09511. doi:[10.1029/2010WR010228](https://doi.org/10.1029/2010WR010228)
- Anderson, E. J., and D. J. Schwab. 2013. Predicting the oscillating bi-directional exchange flow in the Straits of Mackinac. *J. Great Lakes Res.* **39**: 663–671. doi:[10.1016/j.jglr.2013.09.001](https://doi.org/10.1016/j.jglr.2013.09.001)
- Assel, R. A. 2005. Classification of annual Great Lakes ice cycles: Winters of 1973–2002. *J. Climate* **18**: 4895–4905. doi:[10.1175/JCLI3571.1](https://doi.org/10.1175/JCLI3571.1)
- Assel, R., K. Cronk, and D. Norton. 2003. Recent trends in Laurentian Great Lakes ice cover. *Clim. Change* **57**: 185–204. doi:[10.1023/A:1022140604052](https://doi.org/10.1023/A:1022140604052)
- Bai, X., J. Wang, D. J. Schwab, Y. Yang, L. Luo, G. A. Leshkevich, and S. Liu. 2013. Modeling 1993–2008 climatology of seasonal general circulation and thermal structure in the Great Lakes using FVCOM. *Ocean Modell* **65**: 40–63. doi:[10.1016/j.ocemod.2013.02.003](https://doi.org/10.1016/j.ocemod.2013.02.003)
- Bates, G. T., F. Giorgi, and S. W. Hostetler. 1993. Toward the simulation of the effects of the Great Lakes on regional climate. *Mon. Weather Rev.* **121**: 1373–1387. doi:[10.1175/1520-0493\(1993\)121<1373:TTSOTE>2.0.CO;2](https://doi.org/10.1175/1520-0493(1993)121<1373:TTSOTE>2.0.CO;2)
- Beletsky, D., J. H. Saylor, and D. J. Schwab. 1999. Mean circulation in the Great Lakes. *J. Great Lakes Res.* **25**: 78–93. doi:[10.1016/S0380-1330\(99\)70718-5](https://doi.org/10.1016/S0380-1330(99)70718-5)
- Bierman, V. J., Jr., J. Kaur, J. V. DePinto, T. J. Feist, and D. W. Dilks. 2005. Modeling the role of zebra mussels in the proliferation of blue-green algae in Saginaw Bay, Lake Huron. *J. Great Lakes Res.* **31**: 32–55. doi:[10.1016/S0380-1330\(05\)70236-7](https://doi.org/10.1016/S0380-1330(05)70236-7)
- Burwell, D., M. Vincent, M. Luther, and B. Galperin. 2000. Modeling residence times: Eulerian versus Lagrangian, p. 995–1009. *In* M. L. Spaulding and H. L. Butler, [eds.], *Estuarine and coastal modeling*, ASCE.
- Chapra, S. C. 2008. *Surface water-quality modeling*, Wave-land Press.
- Chen, C., H. Liu, and R. C. Beardsley. 2003. An unstructured, finite-volume, three-dimensional, primitive equation ocean model: Application to coastal ocean and estuaries. *J. Atmos. Oceanic Technol.* **20**: 159–186. doi:[10.1175/1520-0426\(2003\)020<0159:AUGFVT>2.0.CO;2](https://doi.org/10.1175/1520-0426(2003)020<0159:AUGFVT>2.0.CO;2)
- Chen, C., and others. 2012. FVCOM model estimate of the location of Air France 447, *Ocean Dynamics*, **62.6** (2012): 943–952.
- Chen, C., and others. 2013. An unstructured, finite-volume, three-dimensional, primitive equation ocean model: FVCOM User Manual, SMAST/UMASSD-13-0701, 4th ed., July 2013.
- Clites, A. H., J. Wang, K. B. Campbell, A. D. Gronewold, R. A. Assel, X. Bai, and G. A. Leshkevich. 2014. Cold water and high ice cover on Great Lakes in spring 2014. *EOS* **95**: 305–306. doi:[10.1002/2014EO340001](https://doi.org/10.1002/2014EO340001)
- Fahnenstiel, G. L., G. A. Lang, T. F. Nalepa, and T. H. Johengen. 1995. Effects of zebra mussel (*Dreissenapoly-morpha*) colonization on water quality parameters in Saginaw Bay, Lake Huron. *J. Great Lakes Res.* **21**: 435–448. doi:[10.1016/S0380-1330\(95\)71057-7](https://doi.org/10.1016/S0380-1330(95)71057-7)
- Fishman, D. B., S. A. Adlerstein, H. A. Vanderploeg, G. L. Fahnenstiel, and D. Scavia. 2009. Causes of phytoplankton changes in Saginaw Bay, Lake Huron, during the zebra mussel invasion. *J. Great Lakes Res.* **35**: 482–495. doi:[10.1016/j.jglr.2009.08.003](https://doi.org/10.1016/j.jglr.2009.08.003)
- Fujisaki, A., J. Wang, H. Hu, D. J. Schwab, N. Hawley, and Y. R. Rao. 2012. A modeling study of ice–water processes for Lake Erie applying coupled ice-circulation models. *J. Great Lakes Res.* **38**: 585–599. doi:[10.1016/j.jglr.2012.09.021](https://doi.org/10.1016/j.jglr.2012.09.021)
- Fujisaki, A., J. Wang, X. Bai, G. Leshkevich, and B. Lofgren. 2013. Model-simulated interannual variability of Lake Erie ice cover, circulation, and thermal structure in response to atmospheric forcing, 2003–2012. *J. Geophys. Res. Oceans* **118**: 4286–4304. doi:[10.1002/jgrc.20312](https://doi.org/10.1002/jgrc.20312)
- Gao, G., C. Chen, J. Qi, and R. C. Beardsley. 2011. An unstructured-grid, finite-volume sea ice model: Development, validation, and application. *J. Geophys. Res. Oceans*. **116**: C00D04. doi:[10.1029/2010JC006688](https://doi.org/10.1029/2010JC006688)
- Ge, Z., R. L. Whitman, M. B. Nevers, M. S. Phanikumar, and M. N. Byappanahalli. 2012. Nearshore hydrodynamics as loading and forcing factors for *Escherichia coli* contamination at an embayed beach. *Limnol. Oceanogr.* **57**: 362–381.
- Gilchrist, T., and P. LaLonde. 2009. Strong winds push ice into beachfront homes along Saginaw Bay [Internet]. The Bay City Times; March 9, 2009, Grand Rapids, Michigan. URL:[http://www.mlive.com/news/saginaw/index.ssf/2009/03/strong\\_winds\\_push\\_ice\\_into\\_bea.html](http://www.mlive.com/news/saginaw/index.ssf/2009/03/strong_winds_push_ice_into_bea.html) [accessed March 11, 2009].
- Gronewold, A. D., and C. A. Stow. 2014. Water loss from the Great Lakes. *Science*. **343**: 1084–1085. doi:[10.1126/science.1249978](https://doi.org/10.1126/science.1249978)
- Hawley, N., T. Redder, R. Beletsky, E. Verhamme, D. Beletsky, and J. V. DePinto. 2014. Sediment resuspension in Saginaw Bay. *J. Great Lakes Res.* **40**: 18–27.
- Heath, R. T., G. L. Fahnenstiel, W. S. Gardner, J. F. Cavaletto, and S. J. Hwang. 1995. Ecosystem-level effects of zebra mussels (*Dreissenapoly-morpha*): An enclosure experiment in Saginaw Bay, Lake Huron. *J. Geophys. Res. Oceans* **21**: 501–516. doi:[10.1016/S0380-1330\(95\)71062-0](https://doi.org/10.1016/S0380-1330(95)71062-0)
- Hecky, R. E., Smith, R. E. D. R. Barton, S. J. Guildford, W. D. Taylor, M. N. Charlton T. Howell., and T. 2004. The near-shore phosphorus shunt: A consequence of ecosystem engineering by dreissenids in the Laurentian Great Lakes. *Can. J. Fish. Aquat. Sci.* **61**: 1285–1293. doi:[10.1139/f04-065](https://doi.org/10.1139/f04-065)
- Hunke, E. C., W. H. Lipscomb, A. K. Turner, N. Jeffery, and S. Elliott. 2013. CICE: The Los Alamos sea ice model, documentation and software user’s manual, Version 5.0, LA-CC-06-012, Los Alamos, NM.
- Marvin, C., S. Painter, and R. Rossmann. 2004. Spatial and temporal patterns in mercury contamination in sediments of the Laurentian Great Lakes. *Environ. Res.* **95**: 351–362. doi:[10.1016/j.envres.2003.09.007](https://doi.org/10.1016/j.envres.2003.09.007)
- Monsen, N. E., J. E. Cloern, L. V. Lucas, and S. G. Monismith. 2002. A comment on the use of flushing

- time, residence time, and age as transport time scales. *Limnol. Oceanogr.* **47**: 1545–1553. doi:[10.4319/lo.2002.47.5.1545](https://doi.org/10.4319/lo.2002.47.5.1545)
- Nakamura, R., O. Takahiro, T. Shibayama, E. Miguel, and H. Takagi. 2015. Evaluation of storm surge caused by typhoon Yolanda (2013) and using weather-storm surge-wave-tide model. *Procedia Eng.* **116**: 373–380. doi:[10.1016/j.proeng.2015.08.306](https://doi.org/10.1016/j.proeng.2015.08.306)
- Nalepa, T. F., D. L. Fanslow, S. A. Pothoven, A. J. Foley III, and G. A. Lang. 2007. Long-term trends in benthic macro-invertebrate populations in Lake Huron over the past four decades. *J. Great Lakes Res.* **33**: 421–436. doi:[10.3394/0380-1330\(2007\)33\[421:LTIBMP\]2.0.CO;2](https://doi.org/10.3394/0380-1330(2007)33[421:LTIBMP]2.0.CO;2)
- Nguyen, T. D. 2014. Circulation and Exchange in the Saginaw Bay – Lake Huron System: Observations and Numerical Modeling. Ph.D. Dissertation, p. 165. UMI Number: 3635531, Department of Civil & Environmental Engineering, Michigan State University, East Lansing, Michigan.
- Nguyen, T. D., P. Thupaki, E. J. Anderson, and M. S. Phanikumar. 2014. Summer circulation and exchange in Saginaw Bay-Lake Huron system. *J. Geophys. Res. Oceans.* **119**: 2713–2734. doi:[10.1002/2014JC009828](https://doi.org/10.1002/2014JC009828)
- Niu, J., C. Shen, S. G. Li, and M. S. Phanikumar. 2014. Quantifying Storage Changes in Regional Great Lakes Watersheds Using a Coupled Subsurface - Land Surface Process Model and GRACE, MODIS products. *Water Resour. Res.* **50**: 7359–7377. doi:[10.1002/2014WR015589](https://doi.org/10.1002/2014WR015589)
- Oveisy, A., L. Boegman, and J. Imberger. 2012. Three-dimensional simulation of lake and ice dynamics during winter. *Limnol. Oceanogr.* **57**: 43. doi:[10.4319/lo.2012.57.1.0043](https://doi.org/10.4319/lo.2012.57.1.0043)
- Rizk, W., G. Kirillin, and M. Lepparanta. 2014. Basin-scale circulation and heat fluxes in ice-covered lakes. *Limnol. Oceanogr.* **59**: 445–464. doi:[10.4319/lo.2014.59.2.0445](https://doi.org/10.4319/lo.2014.59.2.0445)
- Robertson, D. M., R. A. Ragotzkie, and J. J. Magnuson. 1992. Lake ice records used to detect historical and future climatic changes. *Clim. Change* **21**: 407–427. doi:[10.1007/BF00141379](https://doi.org/10.1007/BF00141379)
- Rondy, D. R. 1976. Great Lakes ice cover. In great lakes basin framework study, Appendix 4. Great Lakes Basin Commission, p. 105–118.
- Saylor, J. H., and G. S. Miller. 1976. Winter currents in Lake Huron. NOAA Technical Memorandum ERL GLERL-15.
- Saylor, J. H., and G. S. Miller. 1979. Lake Huron winter circulation. *J. Geophys. Res. Oceans.* **84**: 3237–3252. doi:[10.1029/JC084iC06p03237](https://doi.org/10.1029/JC084iC06p03237)
- Schwab, D. J. 1999. Lake Michigan mass balance study: Hydrodynamic modeling project, NOAA Technical Memorandum ERL GLERL-108.
- Scott, R. W., and F. A. Huff. 1996. Impacts of the Great Lakes on regional climate conditions. *J. Great Lakes Res.* **22**: 845–863. doi:[10.1016/S0380-1330\(96\)71006-7](https://doi.org/10.1016/S0380-1330(96)71006-7)
- Sheng, J., and Y. R. Rao. 2006. Circulation and thermal structure in Lake Huron and Georgian Bay: Application of a nested-grid hydrodynamic model. *Cont. Shelf Res.* **26**: 1496–1518. doi:[10.1016/j.csr.2006.01.019](https://doi.org/10.1016/j.csr.2006.01.019)
- Shore, J. A. 2009. Modelling the circulation and exchange of Kingston Basin and Lake Ontario with FVCOM. *Ocean Model.* **30**: 106–114. doi:[10.1016/j.ocemod.2009.06.007](https://doi.org/10.1016/j.ocemod.2009.06.007)
- Skamarock, W. C., and others. 2008. A description of the advanced research WRF version 3. NCAR technical note, NCAR/TN-475+STR, mesoscale and microscale meteorology division. National Centre for Atmospheric Research.
- Titze, D. J., and J. A. Austin. 2014. Winter thermal structure of Lake Superior. *Limnol. Oceanogr.* **59**: 1336–1348. doi:[10.4319/lo.2014.59.4.1336](https://doi.org/10.4319/lo.2014.59.4.1336)
- Twiss, M. R., D. E. Smith, E. M. Cafferty, and H. J. Carrick. 2014. Phytoplankton growth dynamics in offshore Lake Erie during mid-winter. *J. Great Lakes Res.* **40**: 449–454. doi:[10.1016/j.jglr.2014.03.010](https://doi.org/10.1016/j.jglr.2014.03.010)
- Urrego-Blanco, J., and J. Sheng. 2014. Formation and distribution of sea ice in the Gulf of St. Lawrence: A process-oriented study using a coupled ocean-ice model. *J. Geophys. Res. Oceans.* **119**: 7099–7122. doi:[10.1002/2014JC010185](https://doi.org/10.1002/2014JC010185)
- Van Cleave, K., J. D. Lenters, J. Wang, and E. M. Verhamme. 2014. A regime shift in Lake Superior ice cover, evaporation, and water temperature following the warm El Niño winter of 1997–1998. *Limnol. Oceanogr.* **59**: 1889–1898. doi:[10.4319/lo.2014.59.6.1889](https://doi.org/10.4319/lo.2014.59.6.1889)
- Wang, J., H. Hu, D. J. Schwab, G. Leshkevich, D. Beletsky, N. Hawley, and A. Clites. 2010. Development of the Great Lakes ice-circulation model (GLIM): Application to Lake Erie in 2003–2004. *J. Great Lakes Res.* **36**: 425–436. doi:[10.1016/j.jglr.2010.04.002](https://doi.org/10.1016/j.jglr.2010.04.002)
- Wang, J., and others. 2014. A modeling study of coastal circulation and landfast ice in the nearshore Beaufort and Chukchi seas using CIOM. *J. Geophys. Res. Oceans* **119**: 3285–3312. doi:[10.1002/2013JC009258](https://doi.org/10.1002/2013JC009258)
- Yang, X., Q. Zhang, J. Zhang, F. Tan, Y. Wu, N. Zhang, H. Yang, and Q. Pang. 2015. An integrated model for three-dimensional cohesive sediment transport in storm event and its application on Lianyungang Harbor, China. *Ocean Dynamics.* **65**: 395–417. doi:[10.1007/s10236-014-0806-6](https://doi.org/10.1007/s10236-014-0806-6)

## Acknowledgments

We thank Guoting Kang and Pramod Thupaki for their contributions to this research. Tuan Nguyen's doctoral dissertation research at Michigan State University was made possible by a scholarship from the Vietnam government. This is GLERL Contribution Number 1828.

## Conflict of Interest

None declared.

Submitted 07 July 2015

Revised 11 March 2016; 07 July 2016

Accepted 30 July 2016

Associate editor: Francisco Rueda